PAPER

Check for updates

A novel poly(2-mercaptobenzothiazole) coated magnetic nanoadsorbent derived from ZIF-8 for preconcentration/determination of palladium and silver†

Seyedeh Fatemeh Mohseni,[a] Mahboobeh Manoochehri [ID] *[a] and Faramarz Afshar Taromi[b]

Herein, a novel poly(2-mercaptobenzothiazole) coated magnetic nanoadsorbent derived from zeolitic-imidazole framework-8 (ZIF-8) was synthesized and then employed for the extraction/preconcentration of trace amounts of palladium and silver in various real matrixes. In this way, magnetite was fabricated first, and then functionalized with tetraethyl orthosilicate. After that, the synthesized magnetite@silica was coated with the ZIF-8 to obtain magnetic ZIF-8. Afterward, the magnetic ZIF-8 was pyrolyzed under the protection of a nitrogen atmosphere to get a magnetic carbon nanoadsorbent. Finally, the magnetic carbon was functionalized with a conductive polymer (poly-2-mercaptobenzothiazole). Fabrication of the nanoadsorbent was affirmed with scanning and transmission electron microscopies, elemental analysis, X-ray diffraction, Fourier transform infrared spectroscopy, and vibrating sample magnetometry. The method is linear from 0.25 to 200 μg L^{-1} for silver, and from 0.5 to 250 μg L^{-1} for palladium. The detection limits are 0.07 and 0.15 μg L^{-1} for Ag and Pd, respectively. The precision was evaluated at three concentration levels (1, 75, 200 μg L^{-1}, $n = 5$) and all the relative standard deviation (RSD) values were lower than 10.3%. In the end, the new method was utilized for the preconcentration/determination of trace amounts of palladium and silver in various real matrixes, satisfactorily (relative recovery: 86% to 104%; RSD%: 4.0–9.5%).

1. Introduction

Determination/monitoring of precious metals in solid and liquid waste is a crucial issue from health/environmental and economic points of view.[1] Silver (Ag) as a precious metal is employed in jewelry, medicine, imaging and photographic applications, and fabrication of high corrosion resistance alloys.[2–4] Owing to the extreme application of Ag and its compounds, the concentration of this metal in the environmental samples has been increased.[5]

Palladium (Pd) is another precious metal with application such as catalysts in various manufacturing processes as well as jewelry.[2] Vast amounts of Pd enter the environment as solid waste from discarded automobile catalysts, and chemical industries.[6,7] Therefore, the recovery and monitoring of Ag and

Pd in wastes/environmental samples is a very significant issue in environmental analytical chemistry.[8]

Various instrumental methods including, flame atomic absorption spectrometry (FAAS),[9] graphite furnace atomic absorption spectrometry (GFAAS)[2] and inductively coupled plasma atomic emission spectrometry[10] have been used for the quantification of Ag and Pd. Nonetheless, the mentioned methods cannot be directly employed for environmental samples analysis owing to issues such as the low sensitivity of the most analytical techniques and the complexity of real matrixes. Therefore, an extraction/preconcentration step is mandatory before analyzing real samples.[8]

Diverse sample preparation methods such as solid phase extraction (SPE),[2,11] liquid–liquid extraction,[12] microextraction methods,[13–15] and cloud point extraction[16] have been employed before the determination of Ag and Pd. SPE is the most utilized sample preparation method among the mentioned strategies. This method has various advantages including low consumption of organic solvent, simplicity, sensitivity, and rapidity[4] compared to the LLE method. In this regard, different adsorbs including, alumina,[17] nanoporous silica,[18] Silica gel based chelating sorbent,[19] modified magnetic nanoparticles,[6,11] modified magnetic graphene oxide,[2] and modified carbon

Department of Chemistry, Central Tehran Branch, Islamic Azad University, 1467686831, Tehran, Iran. E-mail: dr.manoochehri@yahoo.com; Fax: +98 2188385798; Tel: +98 9127242698

Department of Polymer Engineering and Color Technology, Amirkabir University of Technology, 424 Hafez Avenue, P. O. Box: 15875-4413, Tehran, Iran

† Electronic supplementary information (ESI) available. See DOI: https://doi.org/10.1039/d2ra06193g

nanotubes[20] have been employed before the quantification of Ag and Pd.

Magnetic solid phase extraction (MSPE) is a new generation of SPE method based on utilizing an adsorbent with super-paramagnetic features.[21] In this approach, the magnetic separation of the adsorbents makes the extraction process faster and easier than the common SPE methods.[22] The bare magnetic nanoparticles (MNPs) has a high tendency to form aggregation, these particles are not selective toward the analytes, and they are not stable in the strong acidic solutions that are mandatory for the desorption of precious metals.[11] Accordingly, the utilization of a support/spacer, and functionalization of MNPs should be performed.[22] Metal–organic frameworks (MOFs), as nanoporous materials, have been reported for this purpose.[8] Zeolitic imidazolate framework-8 (ZIF-8) is a MOF composed of Zn(II) ions as the center and 2-methyl imidazole as an organic linker. ZIF-8 has been utilized for the extraction/ preconcentration of various analytes owing to its high porosity, hydrophobic property, open metal sites, and high stability in aqueous solutions.[23] Recently, MOF-derived magnetic porous carbons (MPCs) have attracted much attention in the MSPE process[22,24] due to their superparamagnetic features including high porosity, high surface area, and tunable structure.[25] In this regard, Asgharinezhad and Ebrahimzadeh utilized a magnetic porous carbon nanocomposite derived from Co-MOF-71 for extraction and determination of homo and hetero-polycyclic aromatic hydrocarbons in various environmental water samples.[24] In another work, a polypyrrole–polythiophene coated magnetic porous carbon nanocomposite derived from Co-MOF-71 was synthesized and utilized for multi-target environmental pollutants preconcentration.[22] Moreover, a bimetallic ZIF-8/ZIF-67 derived porous carbon was synthesized and used as an adsorbent for organochlorine pesticides determination.[26]

Herein, a novel poly(2-mercaptobenzothiazole) coated magnetic nanoadsorbent derived from ZIF-8 was synthesized and then employed for the separation/determination of Pd and Ag in various real matrixes. In this way, magnetite was fabricated first, and then functionalized with tetraethyl orthosilicate. After that, the synthesized magnetite@silica was coated with ZIF-8 to obtain magnetic ZIF-8. Thereafter, the magnetic ZIF-8 was pyrolyzed under the protection of a nitrogen atmosphere to obtain a magnetic carbon nanoadsorbent. Finally, the magnetic carbon was functionalized with a conductive polymer (poly-2-mercaptobenzothiazole) to improve its selectivity toward target metal ions based on the hard and soft and hard acid and base theory.[2] Fabrication of the nanoadsorbent was affirmed with scanning and transmission electron microscopies (SEM and TEM), elemental analysis, X-ray diffraction (XRD), Fourier transform infrared spectroscopy (FT-IE), and vibrating sample magnetometry (VSM). Quantification of the target analytes was performed by a flame atomic absorption spectrometer. There is no report on the synthesis and application of magnetic porous carbon (MPC) nanoadsorbent functionalized with (poly-2-mercaptobenzothiazole) for Ag and Pd determination. The synthesized nanoadsorbent is selective toward Ag and Pd, based on the hard and soft and hard acid and base theory, and

benefits from the superparamagnetic features that accelerate the extraction process. It is worth mentioning that the present study aims to determine the target metals in the real sample.

2. Experimental

2.1. Chemicals

All reagents including $Zn(NO_3)_2 \cdot 6H_2O$, ammonium iron(II) sulfate·$6H_2O$, deionized water, hydrochloric acid, NH_4OH, sulfuric acid, NaOH, nitric acid, tetraethyl orthosilicate (TEOS), thiourea (TU), 2-methyl imidazole (2-mIm), methanol, 2-mercaptobenzothiazole (2-MBT), 1000 mg L^{-1} solutions of Ag(I) and Pd(II), ammonium persulfate (APS), and ethanol with the analytical grade were purchased from Merck (Germany).

2.2. Equipment

Quantification of Ag and Pd was performed on an AA-680 Shimadzu flame atomic absorption spectrometer (Kyoto, Japan) consisting of a C_2H_2–air flame. The radiation sources were hollow cathode lamps (wavelengths: 244.8, for Pd; 328.1 nm for Ag). A morphological study of the nanomaterials was performed on a MIRA3 TESCAN SEM (Czech Republic) and a ZEISS EM90 TEM instrument (Jena, Germany, 80 kV). The FT-IR analysis was accomplished on a spectrophotometer model MB-Series (Bomem, USA). Magnetic features were studied on a VSM instrument model AGFM/VSM117 3886 (Kashan, Iran). XRD tests were performed using a Philips-PW 12C diffractometer (Amsterdam, The Netherlands) with Cu radiation source. Elemental analysis was carried out employing a Thermo Finnigan Flash EA112 apparatus (Okehampton, UK).

2.3. Synthesis process

The fabrication of magnetite@silica was performed based on our former works.[27,28] The synthesis of magnetic ZIF-8 (MZIF-8) was performed as follows: in brief, 0.25 g of magnetite@silica was added to 50 mL methanol and stirred for 30 min. After that, 1.125 g $Zn(NO_3)_2 \cdot 6H_2O$ and 3.1 g 2-mIm were dissolved in 50 mL methanol and added to the suspension.[29] The obtained mixture was moved into an autoclave and heated for 4 h at 50 °C.[29] Finally, the MZIF-8 was magnetically isolated and washed with water (4 × 30 mL) and methanol (4 × 25 mL), and then dried at 60 °C under the vacuum. Next, the MZIF-8 was pyrolyzed at 700 °C for 6 h under the nitrogen atmosphere to achieve MPC.[30] The synthesis of MPC@PMBT was conducted according to our previous report.[31] Briefly, 1.0 g MPC was suspended in 100 mL HCl solution (0.1 mol L^{-1}). After that, 0.335 g of 2-MBT was dissolved in 25 ethanol and then added to the above mixture. After shaking the mixture for 10 min, a 10 mL 0.22 mol L^{-1} aqueous solution of APS was drowsily added to the mixture and the reaction was performed for another 24 h. Eventually, the MPC@PMBT was isolated and washed with methanol and water several times and then dried at ambient temperature. A schematic diagram for the synthesis of MPC@PMBT is lustrated in Fig. 1. Fabrication of the nanoadsorbent was affirmed with SEM, TEM, and elemental analysis, XRD, FTIR and VSM.
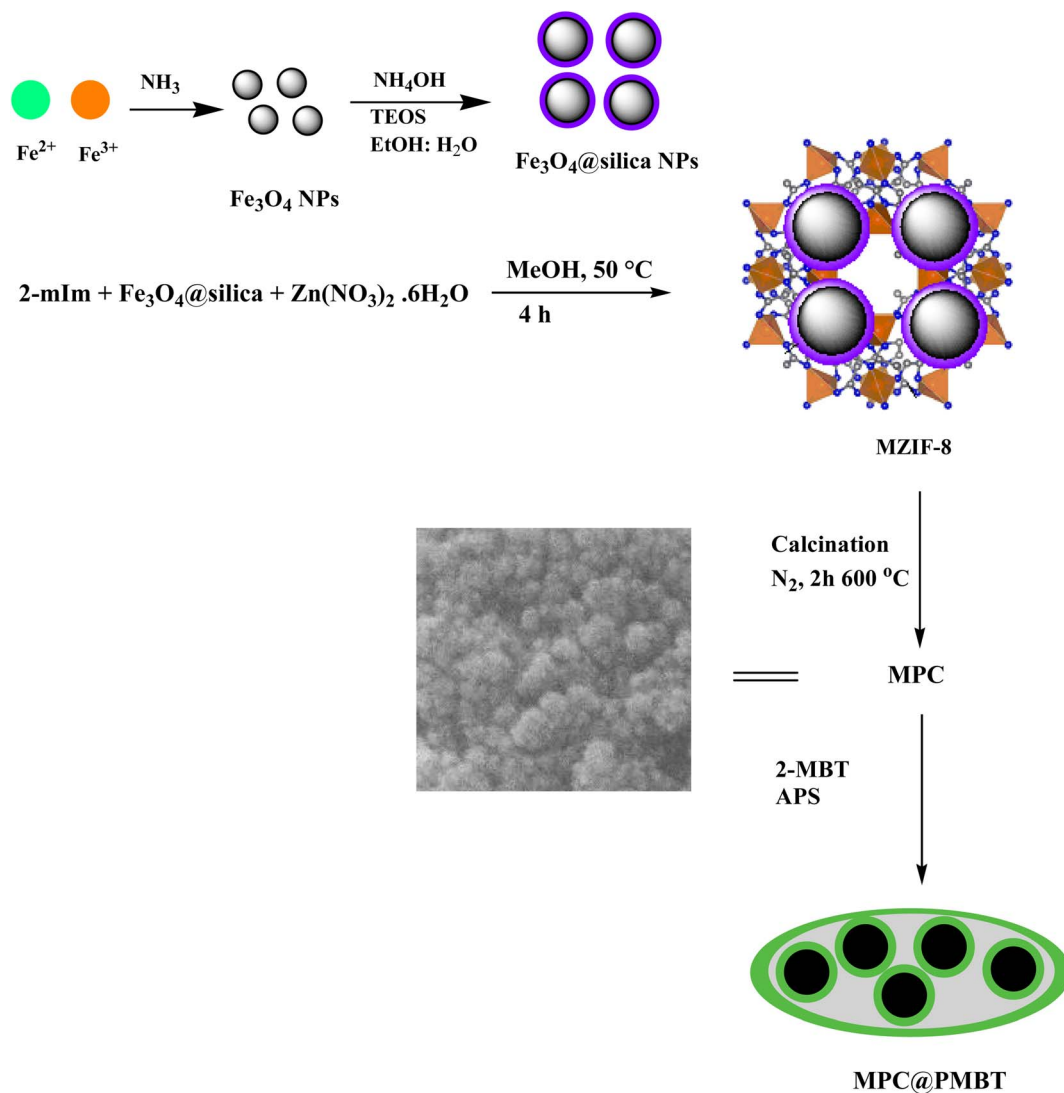
Fig. 1 A scheme for the synthesis of MPC@PMBT nanocomposite.

2.4. MSPE procedure

Firstly, 24 mg of MPC@PMBT was added to 600 mL standard/real sample solution (pH, 6.4; adjusted by 0.1 mol per L NH_4OH and HCl solutions) of the target analytes. After that, the extraction mixture was shaken for 11.5 min and then subjected to a strong permanent magnet for isolation of the MPC@PMBT from the extraction medium and then the supernatant solution was introduced to FAAS to compute the adsorption percentage. In the next step, 1.6 mL eluent consisting 1.0 mol per L TU in 0.15 mol per L HNO_3 solution was added to the MPC@PMBT and the mixture was shaken for 14.5 min. Thereafter, the MPC@PMBT was gathered magnetically and the supernatant solution was introduced to FAAS to compute the elution percentage of Ag and Pd.

2.5. Adsorption capacity

To determine the maximum adsorption capacity (MAC) of the fabricated nanomaterial toward Ag and Pd, standard solutions containing the appropriate concentrations of the target ions were exposed to the MPC@PMBT under optimal conditions. The MAC (mg of adsorbed ions/g of nanoadsorbent) was calculated using the following equation:

$$\text{MAC} = \frac{V}{W}(C_0 - C_e) \tag{1}$$

Herein, MAC is the adsorbed amount of each ion (mg g^{-1}), V represents the sample volume (L), W is the MPC@PMBT weight (g), and C_e and C_0 are the final concentration and initial concentration of metal ions (mg L^{-1}), respectively.

2.6. Real samples

River water (Tehran, Iran) was collected in acid-cleaned polyethylene bottles. Radiological and electroplating wastewater samples were collected in acid-cleaned polyethylene bottles (Qom, Iran).[8] In this regard, the acid-cleaned polyethylene bottles were rinsed 4 times with each water/wastewater sample from the sampling site and then the samples were collected and

immediately were transferred to the laboratory. To keep the target metals in solution until they are analyzed, 5 mL 10% HNO_3 solution was added to one liter of each sample. The road dust sample was collected from a high-traffic area (Tehran, Iran). The water/wastewater samples were filtered before analysis (cellulose membrane, 0.45 μm). One gram of road dust sample was digested with 8 mL concentrated $HCl–HNO_3$ solution 3 : 1 v/v using the following microwave program 2 min at 250 W, no radiation for 2 min, 6 min at 250 W, 5 min at 400 W, 8 min at 550 W, and then venting for 8 min.[8] The residue was diluted in a 100 mL volumetric flask using deionized water. The exact process was accomplished for preparation of the certified reference material (CRM). The pH of all pretreated real samples/CRM was adjusted at 6.4 before performing the extraction process.

2.7. Optimization methodology

In this research, central composite design (CCD) in combination with desirability function (DF) was utilized for simultaneous optimization of the variables in two separate adsorption and elution steps. In the case of multiple response optimization, the Derringer function or DF is utilized.[32] In this way, the response for each analyte is converted to a dimensionless desirability value (d) in the range of 0–1, by dividing each response by the highest response for an individual analyte. After that, the transformed responses are combined into one particular response for each experiment. For a completely undesired response, and a most desirable response d is zero and one, respectively.[32] Based on the $N = 2^f + 2f + C_o$ equation (f: number of factors, C_o: center points), 20 and 30 experiments were designed for adsorption, and elution steps, respectively.[22] Extraction and elution percentages were used as the response factors for the adsorption and elution steps, respectively. Afterward, the response factors were converted to the desirability value in the range of 0–1 for simultaneous optimization of the process for Ag and Pd. Design-Expert software (7.0.0 version) was employed to construct the experiments, and to analyze the obtained data.
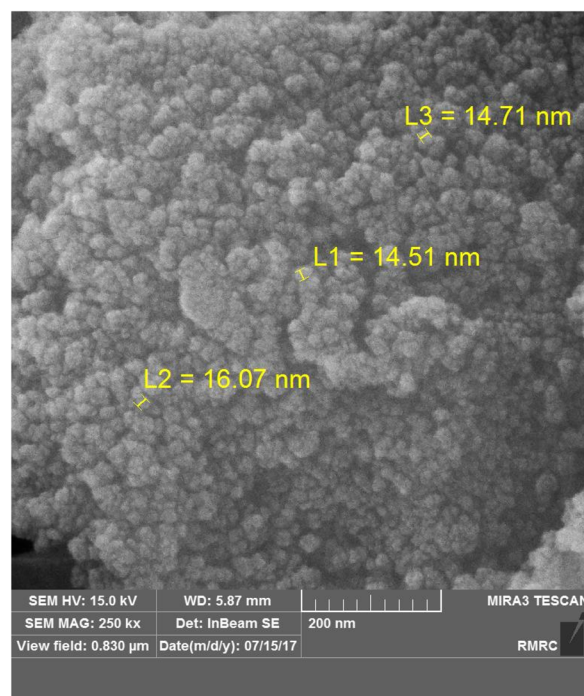
3. Results and discussion

3.1. Characterization

Morphological study of the nanomaterials was carried out by TEM and FE-SEM techniques (Fig. 2). The FE-SEM micrograph (Fig. 2a) of the MPC@PMBT represents a highly porous structure with an average size of 15 nm. The TEM micrograph (Fig. 2b) confirms the results of the FE-SEM analysis. As this figure illustrates, there are regions in the micrograph, an electron-dense region that demonstrates the metal oxides NPs (ZnO, magnetite) and a less dense and more translucent area which can be corresponded to the carbon of MPC and the PMBT coating layer.[26]

CHNS analysis of the MPC@PMBT was performed to determine the percentage of carbon, hydrogen, nitrogen, and sulfur of this nanocomposite. The results revealed the presence of carbon (45.3%), nitrogen (2.9%), hydrogen (1.7%), and sulfur

(a)

L3 = 14.71 nm
L1 = 14.51 nm
L2 = 16.07 nm

SEM HV: 15.0 kV | WD: 5.87 mm | | MIRA3 TESCAN
SEM MAG: 250 kx | Det: InBeam SE | 200 nm |
View field: 0.830 μm | Date(m/d/y): 07/15/17 | | RMRC
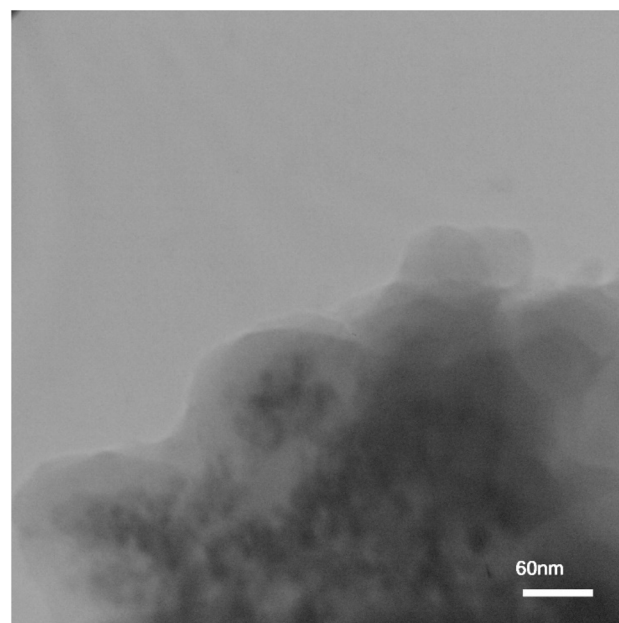
(b)

60nm

Fig. 2 (a) SEM and (b) TEM micrographs of MPC@PMBT composite.

(3.9%) in the composite structure. The presence of sulfur affirms the immobilization of the PMBT layer on the MPC support since only 2-MBT contains the atoms.
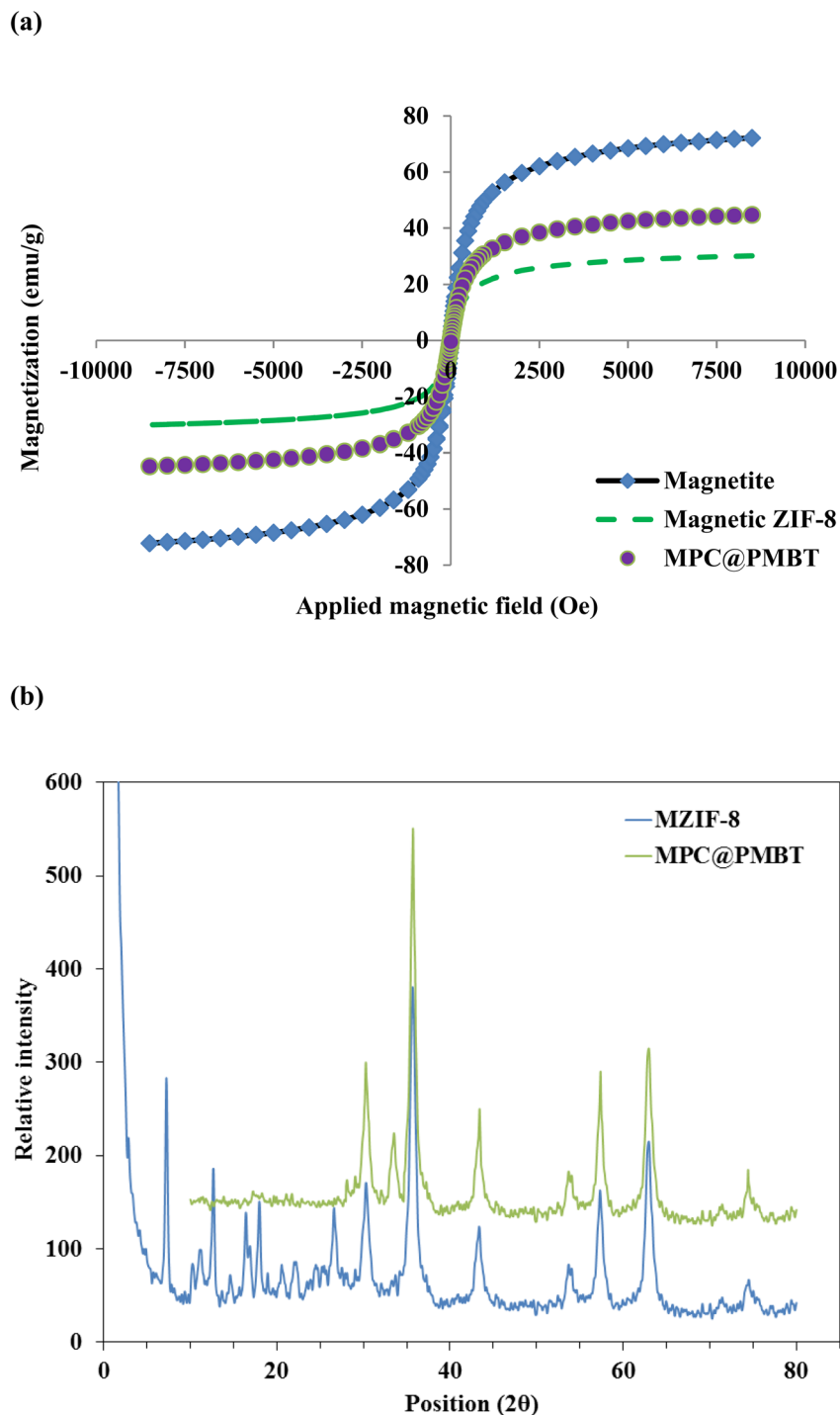
(a)

(b)

Fig. 3 (a) VSM curves Fe_3O_4 NPs, magnetic ZIF-8, and MPC@PMBT composite, (b) XRD patterns of magnetic ZIF-8, and MPC@PMBT composite.

The study of magnetic features of magnetite, MZIF-8, and MPC@PMBT was carried out by the VSM method (Fig. 3a). The saturation magnetization (SM) of magnetite, MZIF-8, and MPC@PMBT was 72.2, 30.1 and 44.7 emu g^{-1}, respectively. The MS values and the hysteresis loop of the curves affirm that all the fabricated materials have superparamagnetic features and hence can be separated easily by employing an external magnet.[33]

The FT-IR spectra of MZIF-8 and MPC@PMBT nano-adsorbents were recorded using the KBr pellet method (Fig. S1, ESI†). The absorption bands at 582 cm^{-1} (Fe–O), 1025 cm^{-1} (Si–O–Si), 1150 cm^{-1} (C–N), and 1535 cm^{-1} (C=C) approve the fabrication of MZIF-8. In the spectrum of MPC@PMBT, the absorption peaks at 580 cm^{-1} (Fe–O), 787 cm^{-1} (C–S), 1028 cm^{-1} (Si–O–Si), 1311 cm^{-1} (C–N), and

Table 1 Experimental variables and levels of the central composite design (CCD)

		Level				
		$-\alpha$	Lower	Central	Upper	$+\alpha$
Sorption step	A: pH of sample	2.64	4.0	6.0	8.0	9.36
	B: MPC@PMBT amount (mg)	9.9	15.0	22.5	30.0	35.1
	C: uptake time (min)	8.3	10.0	12.5	15.0	16.7
Elution step	A: elution time (min)	7.5	10.0	12.5	15.0	17.5
	B: eluent volume (mL)	0.5	1.0	1.5	2.0	2.5
	C: TU concentration (mol L^{-1})	0	0.5	1.0	1.5	2.0
	D: HNO$_3$ concentration (mol L^{-1})	0	0.05	0.1	0.15	0.2

1432 cm^{-1} (C=N) confirm the synthesis of the new nanomaterial.

The phase characterization of MZIF-8 and MPC@PMBT nanomaterials was conducted by the XRD method (Fig. 3b). The characteristics bands of ZIF-8 are visible at $2\theta = 7.2, 12.6, 15.8,$ and 18.5. The characteristic bands of magnetite/ZnO are observable at 30.3, 33.6, 35.7, 43.4, 53.7, 57.4, 63.0, and 74.5 in the structure of MPC@PMBT and confirm the fabrication of MPC.

3.2. Optimization study

3.2.1. Adsorption. In the adsorption process, three affecting factors including, the pH of the sample solution, MPC@PMBT amount, and adsorption time should be optimized (Table 1). Herein, 20 experimental tests were designed based on the CCD method. An F-value as high as 58.27 was obtained for a polynomial quadratic model (Table S1, ESI†), which affirms there is only a 0.01% chance that a model with this large F-value could occur due the noise.[34] The p-value of the constructed model is 0.05 < at 95% confidence level, which proves this model is significant. Besides, the p-value for lack of fit is 0.1341 and there is no pure error in the assay.[24] According to the ANOVA (Table S2†), all the studied factors have a notable effect on the adsorption%. The mathematical model obtained for the optimization of the adsorption step is illustrated in the following equation:

$$\text{Extraction} = +97.39 + 4.29 \times A + 3.55 \times B - 2.91 \times C - 1.07 \times A \times B - 0.57 \times A \times C + 0.18 \times B \times C - 11.00 \times A^2 - 7.80 \times B^2 - 4.47 \times C^2 \quad (2)$$

The adsorption efficiency promotes when the mentioned variables increase according to the Pareto chart (Fig. 4). At the lower pHs the active sites of the MPC@PMBT NPs are protonated and hence the repulsion between metal ions and
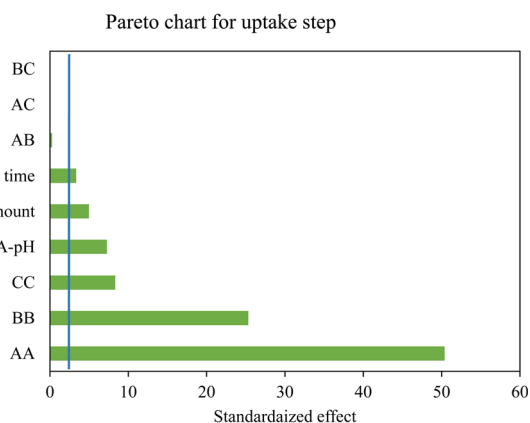

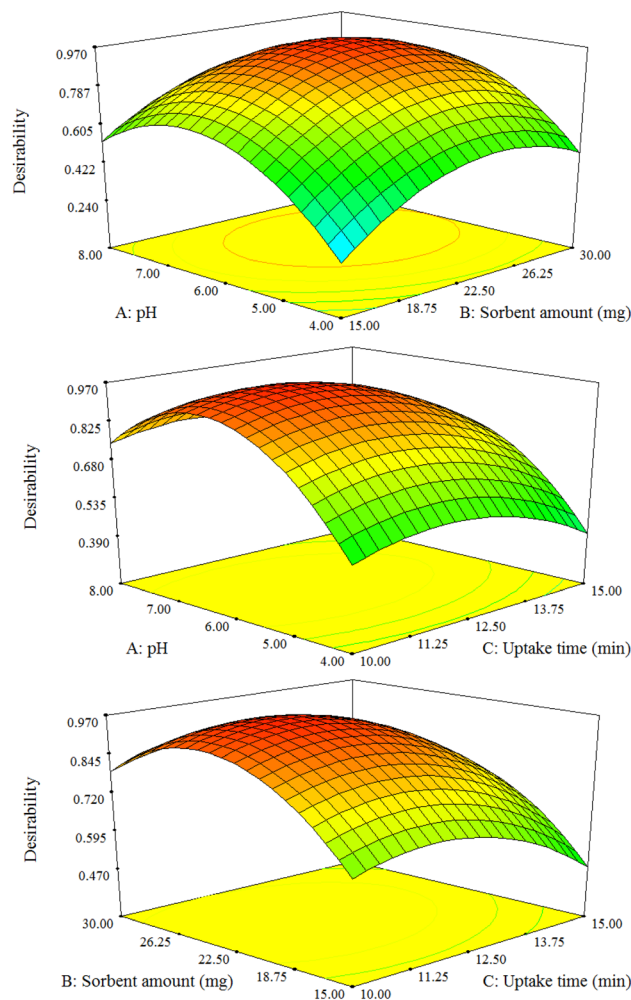**Fig. 4** A Pareto chart for the uptake step.

Fig. 5 3D response surface plots for the adsorption optimization.

protonated heteroatoms is dominant. By increasing the pH, the heteroatoms are deprotonated and coordination interaction occur between the Ag/Pd ions and active sites of the MPC@PMBT.[8,28] Behind the pH value of 6.4 adsorption percentage decreased, which can be due to the competition hydroxide ions to adsorb in the PMBT layer *via* ion-exchange process (Fig. 5). Accordingly, the optimum adsorption condition are: the pH the sample, 6.4; MPC@PMBT dose, 24 mg; adsorption time, 11.5 min.

3.2.2. Elution step. To achieve the complete desorption of the adsorbed analytes from the nanoadsorbent, the application of a suitable eluent is very important in the MSPE method. Accordingly, 0.25 mol L^{-1} solutions of H$_2$SO$_4$, HCl, and HNO$_3$ in 1 mol per L TU were utilized for the desorption process. It is worth noting that the other affecting factors such as the pH of the sample, adsorption time, nanoadsorbent amount, eluent volume and elution time were kept constant at 6.4, 11.5 min, 24 mg, 2 mL and 20 min, respectively. Finally, the best extraction performance was achieved by using 0.25 mol per L HNO$_3$ in 1 mol per L TU solution. After that, the effect of desorption time, HNO$_3$ and TU concentrations, and eluent volume were explored using a CCD strategy. In this way, 30 experiments were accomplished based on the parameters domain summarized in Table 1. The ANOVA results (Table S3†) show an *F*-value of 13.70 (*p*-value < 0.0001), which proves the suggested model is significant and there is only a 0.01% probability that a model with this large *F*-value can occur due the noise.[34] The *p*-value for the lack of fit parameter is 0.2457, which confirms the absence of pure error. The mathematical model obtained for the optimization of the elution parameters is exhibited in the following equation:

$$\text{Recovery (\%)} = +90.29 + 8.23 \times A + 2.83 \times B - 1.43 \times C + 7.81 \times D + 0.12 \times A \times B - 0.15 \times A \times C + 0.71 \times A \times D - 0.083 \times B \times C + 0.78 \times B \times D + 0.50 \times C \times D - 2.17 \times A^2 - 4.56 \times B^2 - 7.34 \times C^2 - 2.61 \times D^2 \quad (3)$$

The result exhibited that the elution time, HNO$_3$ concentration, and eluent volume have significant positive effect on the extraction% of the model ions. In contrast, TU concentration showed a none-significant effect at 95% confidence level (Table S3† and Fig. 6). Moreover, the most significant effect was related to the elution time. Besides, the R^2, and adjusted R^2
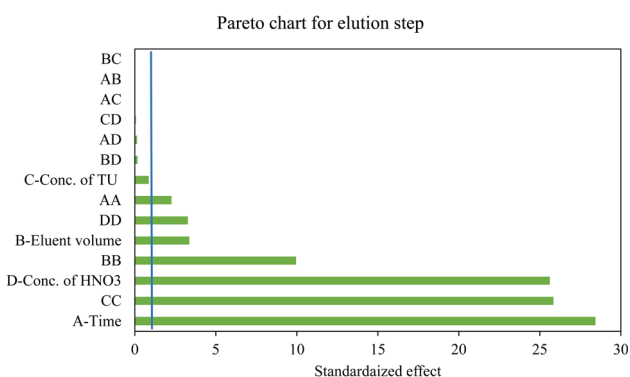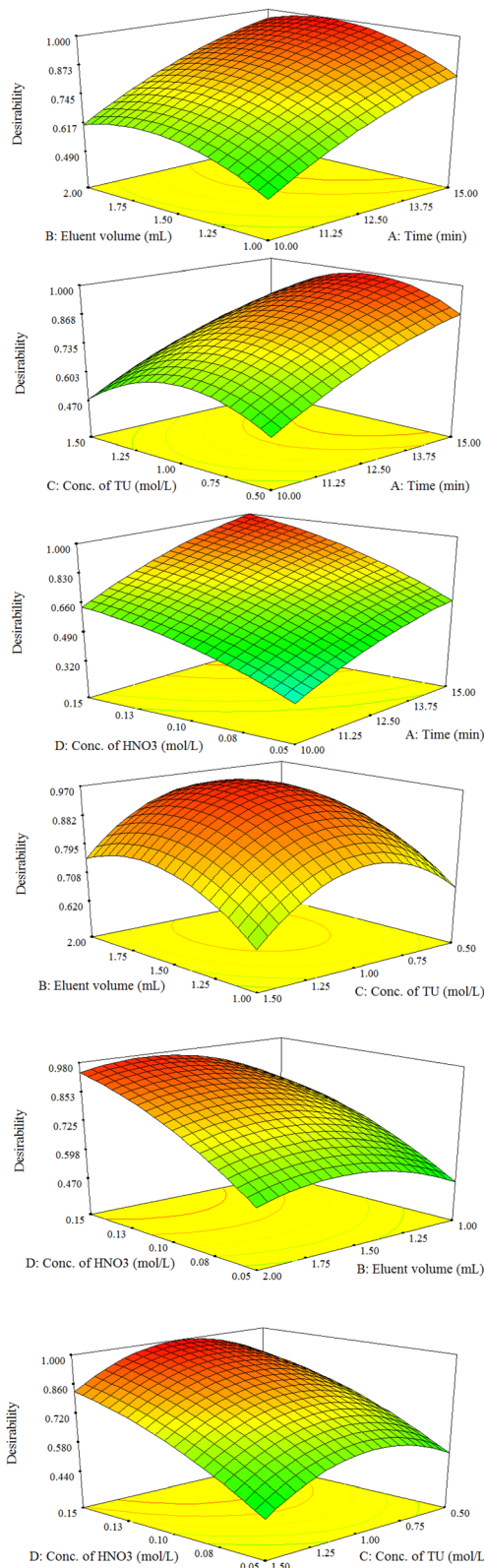

Fig. 6 A Pareto chart for the elution step.

Fig. 7 3D response surface plots for the desorption optimization.

statistical parameters are 0.9275 and 0.8598, respectively and are desirable for a suggested model. The adequate precision parameter as a signal-to-noise ratio measurement should be 4<.

In this study a ratio of 11.766 was obtained indicating a sufficient signal. The response surface plots of the constructed model are illustrated in Fig. 7. A curvature is observable in all the plots, which affirms the parameters are optimized correctly, and depicts the interactions between the parameters.[35] At the end, the optimum desorption conditions are: elution time, 14 min; eluent volume, 1.6 mL; eluent type and concentration, 1.0 mol per L TU in 0.15 mol per L nitric acid.

3.3. Interferences, reusability, and adsorption capacity study

To explore the selectivity of the synthesized nanomaterial and determine the possible interfering species, effect of diverse metal ions was studied (Table 2). The tolerance limit was defined as the concentration of potentially interfering ions that lead to a ±5% deviation in the recovery of the target analytes.[8] The results revealed that the studied interferences have no significant effect on the recovery of Ag and Pd ions as shown in Table 2. Accordingly, it can be concluded that MPC@PMBT nanoadsorbent has a good selectivity for target analytes. Ag(I), and Pd(II) as soft acids tend to interact with the soft bases such as ligands containing S and N atoms, selectively.[2]

The reusability study of MPC@PMBT nanoadsorbent was explored by conducting several adsorption–desorption assays and the recovery of Ag(I) and Pd(II) was determined as an indicator. As exhibited in Fig. S2 (ESI†), the MPC@PMBT can be reused up to 8 tests without considerable decrease in the recovery.

The MAC of MPC@PMBT nanoadsorbent toward Ag and Pd ions was studied by using 100 mL of the standard solution containing an appropriate concentration of each ion. The MAC is defined as the amount of each metal ion (mg) sorbed per

Table 2 Effect of potentially interfering species on the recovery of Ag(I), and Pd(II) ions

Potentially interfering species	Tolerance ratio	Recovery (%), RSD[a]	
		Silver	Palladium
Na^+	25 000	99.3, 4.3	101, 3.9
K^+	25 000	100, 5.1	100, 4.1
Ca^{2+}	12 000	99.8, 4.9	99.4, 5.7
Mg^{2+}	12 000	98.2, 5.3	99.0, 5.5
Cr^{3+}	2000	96.9, 4.2	97.3, 3.5
Fe^{3+}	2000	97.5, 5.0	98.0, 5.0
Mn^{2+}	2000	98.4, 5.4	99.1, 5.4
Al^{3+}	2000	98.0, 3.9	97.5, 4.7
Co^{2+}	1500	98.3, 6.5	98.7, 5.9
Zn^{2+}	1500	97.4, 4.4	97.1, 6.6
Ni^{2+}	800	97.5, 5.6	96.4, 4.6
Pb^{2+}	800	96.0, 4.5	97.2, 6.0
Cd^{2+}	750	95.5, 3.9	96.0, 4.8
Hg^{2+}	250	96.2, 5.0	95.9, 3.5
Cu^{2+}	250	97.1, 6.2	96.6, 5.7
Au^{3+}	400	95.1, 5.3	95.4, 4.4

Conditions: pH, 6.4; uptake time, 11.5 min; MPC@PMBT amount, 24 mg; elution time, 14.5 min; 1.6 mL 1.0 mol per L thiourea in 0.15 mol per L HNO_3 as the eluent. [a] Relative standard deviation.

MPC@PMBT nanoadsorbent weight (g). Accordingly, the MAC for Ag(I) and Pd(II) ions were 153, and 135 mg g^{-1}, respectively.

3.4. Effect of sample volume

The sample volume exhibits a significant effect on the preconcentration factor and hence should be optimized. Accordingly, the effect of sample volume was studied from 100 mL to 750 mL. After that, the preconcentration procedure was accomplished and the recovery of target ions was determined. As depicted in Fig. S3,† quantitative recovery (>90%) of the Ag and Pd ions is achievable up to 600 mL of sample solution. Accordingly, the preconcentration factor (PF) for Ag, and Pd ions was 375 regarding the sample (600 mL) and eluent (1.6 mL) volumes. It is worth to note that an enhancement in the signal was observed when the eluent containing the analytes injected to the FAAS due to the presence of TU in the final solution. In this regard, the calibration plots were obtained with and without the presence of TU for Ag and Pd (Fig. S4, ESI†). The enhancement factor was calculated by dividing the slopes of the calibration plots with and without TU.[7] Accordingly, an enhancement factor of 1.87 and 1.75 was obtained for Ag and Pd, respectively without performing the preconcentration process. As a results the enhancement factors for Ag and Pd are 701 (375 × 1.87), and 656 (375 × 1.75), respectively.

3.5. Analytical figures of merit and comparison study

The analytical figures of merit of the proposed method (linearity, detection limit, precision, recovery) were explored under the optimized extraction conditions. The linearity was achieved in the range of 0.25–200, and 0.5–250 µg L^{-1} with the coefficient of determination (r^2) of 0.9954, and 0.9938 for Ag and Pd, respectively. Detection limit ($3S_b/m$, S_b: the standard deviation of 5 replicates signal of blank sample (deionized water), m: the slope of calibration plots) was 0.07, and 0.15 µg L^{-1} for Ag and Pd, respectively. The repeatability of the method as RSD% values was evaluated at the concentrations of 2.5, 75, and 200 µg L^{-1} ($n = 5$) of Ag and Pd ions. The RSD% values at the concentrations of 2.5, 75, and 200 µg L^{-1} are 10.3%, 7.5% and 4.0%, for Ag ions and 9.9%, 5.8%, and 4.6%, for Pd ions, respectively. These values exhibits the good repeatability of the new method.

The accuracy of the method was evaluated by analyzing 206 BG 326 (ore polymetallic gold Zidarovo-PMZrZ) as a CRM. The obtained concentration for Ag was 17.0 ± 0.2 mg kg^{-1}, which is in good agreement with the certified value (17.2 mg kg^{-1}). Besides, the experimental t-value for the 3 replicates is 1.73, which is lower than critical t-value ($t_{0.05, 2} = 4.30$) and illustrates no significant difference between the experimental value and the real value. Thereby, the optimized method is reliable and accurate for determination of the target ions in real sample analysis complex matrices.

The analytical features of the current research (detection limit, linear range, repeatability, MAC, and PF) was compared to some previously reported methods based on SPE (Table 3). As Tabulated in Table 3, detection limit and repeatability of the current research are better than/comparable with the former

Table 3 Comparison of the features of current method and former adsorbent-based methods for the extraction/determination of palladium and silver

Analytical instrument	Adsorbent	Analyte	LOD (µg L^{-1})	Linear range (µg L^{-1})	PF^a	MAC^b	RSD (%)	Ref.
FAAS	mGO@SiO$_2$@PPy–PTh^c nanocomposite	Ag, Pd	0.1–0.5	0.5–500	112–125	45–49	2.7–4.7	2
ICP-OES^d	Polythiophene-coated Fe$_3$O$_4$ NPs	Ag, Pd	0.2–1.0	0.75–100	87–114	—	3.6–4.2	7
FAAS	MIL-101(Cr)/Fe$_3$O$_4$@SiO$_2$@2-ATP^e nanocomposite	Ag	0.05	0.2–200	294	103	<9.4	8
FAAS	Fe$_3$O$_4$ NPs@murexide	Ag, Pd	0.15–0.25	0.5–400	221–225	34–48	5.0–6.6	11
FI^f-FAAS	Silica gel based chelating sorbent	Ag, Pd	1.3–21	—	15–20	24–30	<3.1	19
FAAS	MPC@PMBT	Ag, Pd	0.07–0.15	0.25–250	375	135–153	<10.3	This research

^{a} Preconcentration factor. ^{b} Maximum adsorption capacity in mg g^{-1}. ^{c} Polypyrrole–polythiophene. ^{d} Inductively coupled plasma optical emission spectrometry. ^{e} 2-Aminothiophenol. ^{f} Flow injection.

Table 4 Palladium and silver determination in the real samples (mean, RSD^a)

Sample	Analyte	Real value, RSD%	Added	Found value, RSD%	Recovery (%)
Radiological wastewater	Ag	185, 5.3	100	273, 4.0	88.0
	Pd	ND^b	10.0	9.0, 7.5	90.0
Road dust^c	Ag	ND	10.0	8.7, 9.2	87.0
	Pd	54.3, 8.2	20.0	71.5, 6.4	86.0
Electroplating wastewater	Ag	149, 6.5	100	245, 5.7	96.0
	Pd	ND	10.0	10.2, 6.3	102
River water	Ag	9.5, 7.8	10.0	19.9, 6.7	104
	Pd	2.1, 9.5	5.0	7.0, 8.0	98.0

All concentrations are based on µg L^{-1} except for road dust sample. ^{a} Relative standard deviation ($n = 3$). ^{b} µg g^{-1}. ^{c} Not detected.

works. The PF value and MAC values for the current method are 300 and 135–153 mg g^{-1}, respectively, which are higher than the former works. Moreover, a wide linear range was achieved compared to the reported works. Another advantage of the current research is using FAAS as a famous, relatively cheap, extensively utilized, and simple to operate detection system.[8]

3.6. Real sample analysis

To confirm the applicability of the current research, several real samples including, river water, road dust, electroplating and photographical wastewaters with various matrix composition were analyzed (Table 4) using the optimized method. Among the analyzed samples, river water, electroplating wastewater, and radiological wastewater exhibited the presence of Ag, while the road dust and river water samples were positive for Pd. To evaluate the accuracy of the method for real sample analysis, spiking of the samples were performed and then the extraction procedure was carried out. As tabulated in Table 4, the recovery values were obtained from 88% to 90% and the repeatability (RSD%) are in the range of 4.0–7.5% for the radiological wastewater sample. The recovery, and RSD% values are 86–87%, and 6.4–9.2% for the road dust sample, while these values for the electroplating wastewater sample are 96–102% and 5.7–6.5%, respectively. Moreover, the recovery, and RSD% values are 98–104%, and 6.7–9.5% for the river water sample, respectively. The obtained results confirm reliability and applicability of the current method for complex matrix samples.

4. Conclusion

Herein, a novel PMBT coated magnetic nanoadsorbent derived from ZIF-8 was synthesized and then employed for the preconcentration/determination of Pd and Ag in various real matrixes. In this way, magnetite was fabricated firstly, and then functionalized with tetraethyl orthosilicate. After that, the synthesized magnetite@silica was coated with a zeolitic-imidazole framework (ZIF) to obtain magnetic ZIF-8. Thereafter, the magnetic ZIF-8 was pyrolized under the protection of a nitrogen atmosphere to obtain a magnetic carbon nano-adsorbent. Finally, the magnetic carbon was functionalized with a conductive polymer (poly-2-mercaptobenzothiazole). There is no report on the synthesis and application of magnetic porous carbon (MPC) nanoadsorbent functionalized with (poly-2-mercaptobenzothiazole) for Ag and Pd preconcentration/determination. The synthesized nano-adsorbent is selective toward Ag and Pd, and benefits from the superparamagnetic features that accelerate the extraction process. High adsorption capacities were obtained in the range of 135–153 mg g^{-1}. The PF was 375 for the target ions and very low LOD values (0.07–0.15 µg L^{-1}) were obtained. The new method exhibited excellent accuracy by analyzing a CRM (206 BG 326). The RSD% values (2.5, 75, and 200 µg L^{-1}) were located in the range of 4.0–10.3% and exhibit the good repeatability of the new method. Eventually, the method was utilized to preconcentration/determination of Ag and Pd in complex

matrices, satisfactorily. The main goal of the current study was determination of the target metals in real sample and the recovery from acidic solution can be investigated in future studies.

Conflicts of interest

There are no conflicts to declare.

References

1 E. Lifshitz, M. Brumer, A. Kigel, A. Sashchiuk, M. Bashouti, M. Sirota, E. Galun, Z. Burshtein, Q. AQLe, I. Ledoux-Rak and J. Zyss, Air-stable PbSe/PbS and PbSe/PbSexS1-x core-shell nanocrystals quantum dots and their applications, *J. Phys. Chem. B*, 2006, **110**, 25356–25365.

2 N. Jalilian, H. Ebrahimzadeh, A. A. Asgharinezhad and K. Molaei, Extraction and determination of trace amounts of gold (III), palladium (II), platinum (II) and silver (I) with the aid of a magnetic nanosorbent made from Fe3O4-decorated and silica-coated graphene oxide modified with a polypyrrole-polythiophene copolymer, *Microchim. Acta*, 2017, **184**(7), 2191–2200.

3 T. Rohani and M. A. Taher, Preparation of a carbon ceramic electrode modified by 4-(2-pyridylazo)-resorcinol for determination of trace amounts of silver, *Talanta*, 2010, **80**(5), 1827–1831.

4 T. Çetin, Ş. Tokalıoğlu, A. Ülgen, S. Şahan, İ. Özentürk and C. Soykan, Synthesis/characterization of a new chelating resin and on-line solid phase extraction for the determination of Ag (I) and Pd (II) from water, cream, anode slime and converter samples by flow injection flame atomic absorption spectrometry, *Talanta*, 2013, **105**, 340–346.

5 C. K. Christou and A. N. Anthemidis, Flow injection on-line displacement/solid phase extraction system coupled with flame atomic absorption spectrometry for selective trace silver determination in water samples, *Talanta*, 2009, **78**(1), 144–149.

6 K. Jarvis, S. Parry and J. Piper, Temporal and spatial studies of autocatalyst derived platinum, rhodium, and palladium and selected vehicle-derived trace elements in the environment, *Environ. Sci. Technol.*, 2001, **35**, 1031–1036.

7 E. Tahmasebi and Y. Yamini, Polythiophene-coated Fe3O4 nanoparticles as a selective adsorbent for magnetic solid-phase extraction of silver(I), gold(III), copper(II) and palladium(II), *Microchim. Acta*, 2014, **181**, 543–551.

8 S. H. Mousavi, M. Manoochehri and F. A. Taromi, Fabrication of a novel magnetic metal–organic framework functionalized with 2-aminothiophenol for preconcentration of trace silver amounts in water and wastewater, *RSC Adv.*, 2021, **11**(23), 13867–13875.

9 H. Ebrahimzadeh, N. Shekari, N. Tavassoli, M. M. Amini, M. Adineh and O. Sadeghi, Extraction of trace amounts of silver on various amino-functionalized nanoporous silicas in real samples, *Microchim. Acta*, 2010, **170**, 171–178.

10 L. Tavakoli, Y. Yamini, H. Ebrahimzadeh, A. Nezhadali, S. Shariati and F. Nourmohammadian, Development of cloud point extraction for simultaneous extraction and determination of gold and palladium using ICP-OES, *J. Hazard. Mater.*, 2008, **152**, 737–743.

11 S. Karami, H. Ebrahimzadeh and A. A. Asgharinezhad, A simple and fast method based on functionalized magnetic nanoparticles for the determination of Ag (i), Au (iii) and Pd (ii) in mine stone, road dust and water samples, *Anal. Methods*, 2017, **9**(19), 2873–2882.

12 E. Lachowicz, B. Różańska, F. Teixidor, H. Meliani, M. Barboiu and N. Hovnanian, Comparison of sulphur and sulphur–oxygen ligands as ionophores for liquid–liquid extraction and facilitated transport of silver and palladium, *J. Membr. Sci.*, 2002, **210**(2), 279–290.

13 Z. A. ALOthman, M. A. Habila, E. Yilmaz, E. A. Alabdullkarem and M. Soylak, A novel deep eutectic solvent microextraction procedure for enrichment, separation and atomic absorption spectrometric determination of palladium at ultra-trace levels in environmental samples, *Measurement*, 2020 Mar 1, **153**, 107394.

14 A. G. Moghadam, M. Rajabi, M. Hemmati and A. Asghari, Development of effervescence-assisted liquid phase microextraction based on fatty acid for removaltion of silver and cobalt ions using micro-sampling flame atomic absorption spectrometry, *J. Mol. Liq.*, 2017, **242**, 1176–1183.

15 M. Ezoddin, K. Abdi and N. Lamei, Development of air assisted liquid phase microextraction based on switchable-hydrophilicity solvent for the determination of palladium in environmental samples, *Talanta*, 2016, **153**, 247–252.

16 M. Ghaedi, A. Shokrollahi, K. Niknam, E. Niknam, A. Najibi and M. Soylak, Cloud point extraction and flame atomic absorption spectrometric determination of cadmium (II), lead (II), palladium (II) and silver (I) in environmental samples, *J. Hazard. Mater.*, 2009, **168**(2–3), 1022–1027.

17 M. A. Taher, Z. Daliri and H. Fazelirad, Simultaneous extraction and preconcentration of copper, silver and palladium with modified alumina and their determination by electrothermal atomic absorption spectrometry, *Chin. Chem. Lett.*, 2014, **25**(4), 649–654.

18 M. Behbahani, F. Najafi, M. M. Amini, O. Sadeghi, A. Bagheri and P. G. Hassanlou, Solid phase extraction using nanoporous MCM-41 modified with 3, 4-dihydroxybenzaldehyde for simultaneous preconcentration and removal of gold (III), palladium (II), copper (II) and silver (I), *J. Ind. Eng. Chem.*, 2014, **20**(4), 2248–2255.

19 P. Liu, Q. Pu and Z. Su, Synthesis of silica gel immobilized thiourea and its application to the on-line preconcentration and separation of silver, gold and palladium, *Analyst*, 2000, **125**(1), 147–150.

20 M. Ghaedi, M. Montazerozohori, E. Nazari and R. Nejabat, Functionalization of multiwalled carbon nanotubes for the solid-phase extraction of silver, cadmium, palladium, zinc, manganese and copper by flame atomic absorption spectrometry, *Hum. Exp. Toxicol.*, 2013, **32**(7), 687–697.

21 A. A. Asgharinezhad, H. Ebrahimzadeh, M. Rezvani, N. Shekari and M. Loni, A novel 4-(2-pyridylazo) resorcinol functionalised magnetic nanosorbent for selective extraction of Cu (II) and Pb (II) ions from food and water samples, *Food Addit. Contam., Part A*, 2014, **31**(7), 1196–1204.

22 A. A. Asgharinezhad and H. Ebrahimzadeh, A novel polymer coated magnetic porous carbon nanocomposite derived from a metal-organic framework for multi-target environmental pollutants preconcentration, *J. Chromatogr. A*, 2020, **1634**, 461664.

23 X. Liu, Z. Sun, G. Chen, W. Zhang, Y. Cai, R. Kong, X. Wang, Y. Suo and J. You, Determination of phthalate esters in environmental water by magnetic Zeolitic Imidazolate Framework-8 solid-phase extraction coupled with high-performance liquid chromatography, *J. Chromatogr. A*, 2015, **1409**, 46–52.

24 A. A. Asgharinezhad and H. Ebrahimzadeh, Magnetic porous carbon nanocomposite derived from cobalt based-metal-organic framework for extraction and determination of homo and hetero-polycyclic aromatic hydrocarbons, *Talanta*, 2021, **233**, 122526.

25 S. D. Davari, M. Rabbani, A. A. Basti and M. K. Koohi, Determination of furfurals in baby food samples after extraction by a novel functionalized magnetic porous carbon, *RSC Adv.*, 2022, **12**(33), 21181–21190.

26 Y. Liu, Z. Gao, R. Wu, Z. Wang, X. Chen and T. W. D. Chan, Magnetic porous carbon derived from a bimetallic metal–organic framework for magnetic solid-phase extraction of organochlorine pesticides from drinking and environmental water samples, *J. Chromatogr. A*, 2017, **1479**, 55–61.

27 S. Rezabeyk and M. Manoochehri, Selective extraction and determination of beryllium in real samples using amino-5, 8-dihydroxy-1, 4-naphthoquinone functionalized magnetic MIL-53 as a novel nanoadsorbent, *RSC Adv.*, 2020, **10**(60), 36897–36905.

28 M. Mehraban, M. Manoochehri and F. A. Taromi, Trace amount determination of Cd (II), Pb (II) and Ni (II) ions in agricultural and seafood samples after magnetic solid phase extraction by MIL-101 (Cr)/phenylthiosemicarbazide-functionalized magnetite nanoparticle composite, *New J. Chem.*, 2018, **42**(21), 17636–17643.

29 H. Lan, N. Gan, D. Pan, F. Hu, T. Li, N. Long, H. Shen and Y. Feng, Development of a novel magnetic molecularly imprinted polymer coating using porous zeolite imidazolate framework-8 coated magnetic iron oxide as carrier for automated solid phase microextraction of estrogens in fish and pork samples, *J. Chromatogr. A*, 2014, **1365**, 35–44.

30 Y. Liu, Z. Gao, R. Wu, Z. Wang, X. Chen and T. W. Chan, Magnetic porous carbon derived from a bimetallic metal–organic framework for magnetic solid-phase extraction of organochlorine pesticides from drinking and environmental water samples, *J. Chromatogr. A*, 2017, **1479**, 55–61.

31 M. Sohaniyan, M. Manoochehri and M. Daghighi Asli, Liquid chromatographic determination of trace levels of nitrophenols in water samples after dispersive magnetic solid phase extraction, *J. Sep. Sci.*, 2019, **42**(23), 3528–3534.

32 A. A. Asgharinezhad and H. Ebrahimzadeh, Coextraction of acidic, basic and amphiprotic pollutants using multiwalled carbon nanotubes/magnetite nanoparticles@ polypyrrole composite, *J. Chromatogr. A*, 2015, **1412**, 1–11.

33 N. Jalilian, H. Ebrahimzadeh and A. A. Asgharinezhad, Preparation of magnetite/multiwalled carbon nanotubes/metal-organic framework composite for dispersive magnetic micro solid phase extraction of parabens and phthalate esters from water samples and various types of cream for their determination with liquid chromatography, *J. Chromatogr. A*, 2019, **1608**, 460426.

34 N. Jalilian, H. Ebrahimzadeh and A. A. Asgharinezhad, Determination of acidic, basic and amphoteric drugs in biological fluids and wastewater after their simultaneous dispersive micro-solid phase extraction using multiwalled carbon nanotubes/magnetite nanoparticles@ poly (2-aminopyrimidine) composite, *Microchem. J.*, 2018, **143**, 337–349.

35 S. Seidi and M. Fotouhi, Magnetic dispersive solid phase extraction based on polythiophene modified magnetic graphene oxide for mercury determination in seafood followed by flow-injection cold vapor atomic absorption spectrometry, *Anal. Methods*, 2017, **9**(5), 803–813.